

# Discontinuous transition from direct to inverse cascade in three-dimensional turbulence\*

Ganapati Sahoo<sup>1</sup>, Alexandros Alexakis<sup>2</sup> and Luca Biferale<sup>1</sup>

<sup>1</sup> *Department of Physics and INFN, University of Rome 'Tor Vergata',  
Via della Ricerca Scientifica 1, 00133 Rome, Italy. and*

<sup>2</sup> *Laboratoire de Physique Statistique, École Normale Supérieure, CNRS,  
Université Pierre et Marié Curie, Université Paris Diderot, 24 rue Lhomond, 75005 Paris, France.*

Inviscid invariants of flow equations are crucial in determining the direction of the turbulent energy cascade. In this work we investigate a variant of the three-dimensional Navier-Stokes equations that shares exactly the same ideal invariants (energy and helicity) and the same symmetries (under rotations, reflections and scale transforms) as the original equations. It is demonstrated that the examined system displays a change in the direction of the energy cascade when varying the value of a free parameter which controls the relative weights of the triadic interactions between different helical Fourier modes. The transition from a forward to inverse cascade is shown to occur at a critical point in a discontinuous manner with diverging fluctuations close to criticality. Our work thus supports the observation that purely isotropic and three-dimensional flow configurations can support inverse energy transfer when interactions are altered and that inside all turbulent flows there is a competition among forward and backward transfer mechanisms which might lead to multiple energy-containing turbulent states.

In turbulence the energy cascade direction determines the macroscopic properties of the flow, leading to a finite energy dissipation rate in the case of a forward cascade (from large to small scales) or to the formation of a condensate in the case of an inverse cascade (from small to large scales) [1]. It has been long thought that the cascade direction is determined by the dimensionality and by the ideal invariants of the flow. Two-dimensional turbulence possesses two sign definite invariants, the energy and the enstrophy. Energy is transferred backward to larger scales while enstrophy is transferred forward to the small scales. In 3D turbulence, energy is sign definite, while the second invariant, the helicity, is sign indefinite. As a result, helicity does not impose any local or global constraints and it is an empirical fact that in 3D turbulent flows both energy and helicity are transferred to small scales [2, 3].

Other systems develop a more complex phenomenology; e.g., flows in thin layers, in a stratified medium, in the presence of rotation or of magnetic field show a quasi-2D behavior [4–13] and display a bidirectional split energy cascade: part of the energy goes towards small scales (as in 3D) and part to the large scales (as in pure 2D flows). This phenomenon has also been observed in recent experiments [14–16] and in atmospheric measurements [17]. The reason for the appearance of an inverse energy flux is ascribed to the presence of (resonant) waves or of geometric confinement that favor the enhancement of quasi-2D Fourier interactions over the 3D background.

In this work we study a model system for which the interactions in the Navier-Stokes equations (NSE) are en-

hanced or suppressed in a controlled way without reducing the number of degrees of freedom, altering the inviscid invariants or breaking any of the symmetries of the NSE. Our study is based on the helical decomposition [18–21] of the velocity field  $\mathbf{u}$ , that in terms of its Fourier modes  $\tilde{\mathbf{u}}_{\mathbf{k}}$  is written as  $\tilde{\mathbf{u}}_{\mathbf{k}} = \tilde{u}_{\mathbf{k}}^+ \mathbf{h}_{\mathbf{k}}^+ + \tilde{u}_{\mathbf{k}}^- \mathbf{h}_{\mathbf{k}}^-$ , where  $\mathbf{h}_{\mathbf{k}}^{\pm}$  are the eigenvectors of the curl operator  $i\mathbf{k} \times \mathbf{h}_{\mathbf{k}}^{\pm} = \pm k \mathbf{h}_{\mathbf{k}}^{\pm}$ . In real space the velocity field is written as  $\mathbf{u} = \mathbf{u}^+ + \mathbf{u}^-$  where  $\mathbf{u}^{\pm}$  is the velocity field whose Fourier transform is projected to the  $\mathbf{h}^{\pm}$  base. It is easy to realize that, in terms of the helical decomposition, the nonlinear term of the 3D NSE is split in 4 (8 by considering the obvious symmetry that changes the sign of all helical modes) possible classes of helical interactions, corresponding to triads of helical Fourier modes,  $(\tilde{u}_{\mathbf{k}}^{\pm}, \tilde{u}_{\mathbf{q}}^{\pm}, \tilde{u}_{\mathbf{p}}^{\pm})$ , as depicted by the four triadic families in Fig. 1. In our simula-

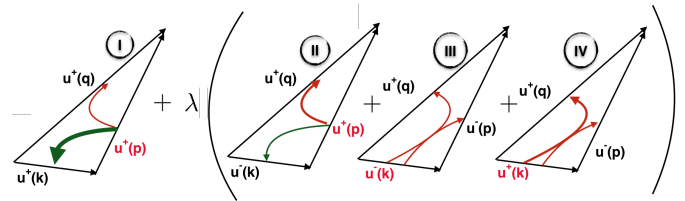


FIG. 1: Sketch of the four classes of the helical-Fourier decomposition of NSE. Green (red) lines describe the backward (forward) energy transfer from the most unstable mode [21]. The thicker line corresponds to the dominant term.

tions we change the relative weight among homochiral triads (Class I) and all the others by introducing a factor  $0 \leq \lambda \leq 1$  in the nonlinear evolution. We show that by using this weighting protocol the turbulent evolution displays a sharp transition, for a critical value  $\lambda_c$ , from forward to backward energy transfer but still keep-

\*Postprint version of the manuscript published in Phys. Rev. Lett. **118**, 164501 (2017)

ing the dynamics fully three-dimensional, isotropic, and parity invariant. It was shown in Ref. [21] that a generic single homochiral triad (from Class I in Fig. 1) always leads to an excess of energy transfer to large scales. The transfer direction of triads of Class-II depends on the geometry of the three interacting modes while Class III and IV always transfer energy forward. In Refs. [22, 23] it was shown that if the NSE is restricted to all homochiral interactions (Class I) it displays a fully isotropic 3D inverse energy cascade. In Ref. [24], a system that transitioned from the NSE to that of homochiral triads [22, 23] was investigated by introducing a random decimation of modes with negative helicity with a varying probability,  $0 \leq \alpha \leq 1$  ( $\alpha = 0$  being the original NSE and  $\alpha = 1$  being the system of homochiral triads). In that study, the transition from forward to inverse energy cascade happens in a quasi-singular way such that the inverse cascade exists only at  $\alpha \sim 1$  demonstrating that even if only a small set of interactions among helical waves of both sign are present (Class II, III and IV), the energy transfer is always forward. Similar conclusions were reached in Ref. [25] where the amplitude of the negative helical modes was controlled by a dynamical forcing.

In this work we investigate a variant of the original NSE obtained by introducing different weighting of the 4 helical-Fourier classes, such as to smoothly interpolate from the full NSE to the reduced version [22, 23] where interactions among the  $\mathbf{u}^+$  and the  $\mathbf{u}^-$  are forbidden, but without removing any modes. In particular, we evolve the following system:

$$\partial_t \mathbf{u} = \mathbb{P}[\mathcal{N}] - \nu \Delta^4 \mathbf{u} - \mu \Delta^{-2} \mathbf{u} + \mathbf{F} \quad (1)$$

where  $\nu$  is the coefficient of the hyperviscosity term and  $\mu$  is the coefficient of the energy sink at large scale needed to arrest the inverse cascade of energy (if any).  $\mathbb{P}$  is a projection operator to incompressible fields. The nonlinearity  $\mathcal{N}$  is defined as  $\mathcal{N} = \lambda(\mathbf{u} \times \mathbf{w}) + (1 - \lambda)[\mathbb{P}^+(\mathbf{u}^+ \times \mathbf{w}^+) + \mathbb{P}^-(\mathbf{u}^- \times \mathbf{w}^-)]$ , where  $\mathbf{w} = \nabla \times \mathbf{u}$  is the vorticity, and  $\mathbb{P}^\pm$  stands for the projection operator to the incompressible helical base with  $\mathbf{u}^\pm = \mathbb{P}^\pm[\mathbf{u}]$  and  $\mathbb{P} = \mathbb{P}^+ + \mathbb{P}^-$ . This model, proposed in Ref. [26], is graphically summarized in Fig. 1. For any value of  $\lambda$  the inviscid system conserves the same quantities as the 3D NSE, namely, the energy  $E = \frac{1}{2} \langle \mathbf{u}^2 \rangle$  and the helicity  $H = \frac{1}{2} \langle \mathbf{u} \cdot \mathbf{w} \rangle$  (where the angle brackets stand for spatial average), and has the same rotation, reflection, and dilatation symmetries. For  $\lambda = 1$ ,  $\mathcal{N}$  reduces to the nonlinearity of the NSE and energy cascades forward. For  $\lambda = 0$  the two fields  $\mathbf{u}^\pm$  decouple and Eq.(1) becomes the equation examined in Refs. [22, 23]. It conserves two energies  $E^\pm = \frac{1}{2} \langle (\mathbf{u}^\pm)^2 \rangle$  and two sign definite helicities  $H^\pm = \frac{1}{2} \langle \mathbf{u}^\pm \cdot \mathbf{w}^\pm \rangle$  independently and cascades energy inversely. We thus expect that as  $\lambda$  is varied continuously from  $\lambda = 1$  to  $\lambda = 0$  there will be a change in the direction of energy cascade from forward to inverse. The purpose of this work is to investigate how this transition takes place as the parameter  $\lambda$  is

Run	$N$	$k_f$	$\nu$	$\mu$	$Re$
N1K1	256	[10, 12]	$10^{-14}$	0.5	$6 \times 10^6$
N2K1	512	[10, 12]	$10^{-16}$	0.5	$6 \times 10^8$
N3K1	1024	[10, 12]	$10^{-18}$	0.5	$6 \times 10^{10}$
N2K2	512	[20, 22]	$10^{-16}$	0.5	$5 \times 10^6$

TABLE I: Values of the parameters used in the DNS.  $N$ , spatial resolution;  $k_f$ , forcing range;  $\nu$ , viscosity;  $Re = \varepsilon_{inj}^{1/3} / (\nu k_f^{2/3})$  is the Reynolds number. The large-scale friction  $\mu$  is applied for only  $k < k_\mu = 2$ .

varied. We perform a systematic series of high resolution numerical simulations of Eq. (1) in a box of size  $L = 2\pi$ . Energy is injected at intermediate wavenumbers  $k_f$  by a Gaussian white-in-time forcing with a fixed injection rate  $\varepsilon_{inj}$ . We use a pseudo-spectral code, fully dealiased and with second order Adams-Bashforth time advancing scheme with exact integration of the viscous term. Table I lists the parameters for all simulations.

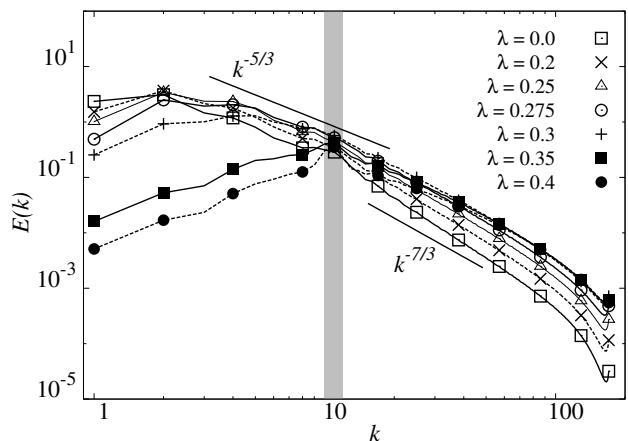


FIG. 2: Log-log plot of energy spectra at changing  $\lambda$  and for fixed forcing range (runs N2K1 in Table I). The gray area denotes the forcing window. The two straight lines correspond to the scaling predicted in the presence of an energy cascade and for the helicity cascade. For  $\lambda > \lambda_c \sim 0.3$ , there is no inverse energy cascade and  $E(k) \propto k^{-5/3}$ . For  $\lambda < \lambda_c$ , we have an inverse energy transfer and a forward helicity transfer,  $E(k) \propto k^{-7/3}$ .

Figure 2 shows the energy spectra measured at the steady state for different values of the parameter  $\lambda$  obtained from simulations N2K1. Clearly, for large values of  $\lambda$  there is no significant energy in the large scales, while small scales display a spectrum compatible with  $k^{-5/3}$ . For small values of  $\lambda$ , the energy is peaked at large scales forming a spectrum close to  $k^{-5/3}$ , while a steeper spectrum closer to  $k^{-7/3}$  is observed in the small scales. The two behaviors suggest a change from a forward to an inverse cascade, which is best demonstrated by looking at the energy fluxes depicted in Fig. 3. The energy

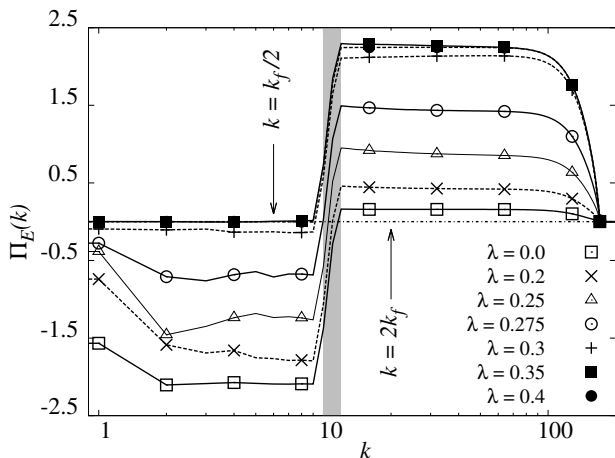


FIG. 3: Energy flux for different values of  $\lambda$ . The gray band shows the forced range of wavenumbers. The arrows mark the wavenumbers at which we measure the fluctuations in the flux (see insets of Fig. 4).

flux is defined as  $\Pi(k) = -\langle \mathbf{u}_k^< \cdot \mathcal{N} \rangle$ , where  $\mathbf{u}_k^<$  expresses the velocity field  $\mathbf{u}$  filtered so that its Fourier transform contains only wavenumbers  $\mathbf{k}$  satisfying  $|\mathbf{k}| \leq k$ , and expresses that the rate energy is transferred out of the set of wavenumbers  $|\mathbf{k}| \leq k$  to larger  $\mathbf{k}$ .  $\Pi(k)$  is constant in the inertial ranges  $k_\mu \ll k \ll k_f$  and  $k_f \ll k \ll k_\nu$  (where  $k_\mu \sim 1$  is the hypoviscous wavenumber and  $k_\nu \sim N/3$  the viscous-wavenumber). It is positive if the cascade is direct and negative if the cascade is inverse.

As  $\lambda$  is varied the direction of cascade is changing. For  $\lambda \geq 0.3$  the flux is almost zero for  $k < k_f$ , while it is positive and constant for  $k_f < k < k_\nu$ . For  $\lambda \leq 0.2$  the opposite picture holds. For  $k < k_f$  the flux is negative and constant, while for  $k > k_f$  the flux is positive but weak. For values of  $\lambda$  in the range  $0.2 < \lambda < 0.3$ , we observe a bidirectional cascade: the coexistence of a forward and inverse transfer. Let us notice that the transition happens close to  $\lambda = 1/3$  that corresponds to the case where the weight of homochiral triads equals the cumulative weight of all heterochiral ones.

The bidirectional cascade is, however, a finite size effect and this behavior does not survive the large Reynolds number and the large box-size limits, as shown in Fig. 4. The inverse flux (measured at the wavenumber  $k = k_f/2$ ) as a function of  $\lambda$  for different values of the Reynolds numbers (grid sizes) and different box sizes is shown in Fig. 4(a) while the forward energy flux (measured at the wavenumber  $k = 2k_f$ ) is shown in Fig. 4(b). Both fluxes are normalized by the total injection rate  $\varepsilon_{inj}$ . The different symbols correspond to an increase of  $Re$  keeping  $k_f$  fixed (runs N1K1  $\rightarrow$  N2K1  $\rightarrow$  N3K1) or to an increase of  $k_f$  keeping  $Re$  approximately fixed (runs N1K1  $\rightarrow$  N2K2). For run N1K1 the transition from forward to inverse cascade is smooth, displaying a bidirectional cascade for values of  $\lambda$  in the range  $0 < \lambda < \lambda_c \simeq 0.3$ , while a pure for-

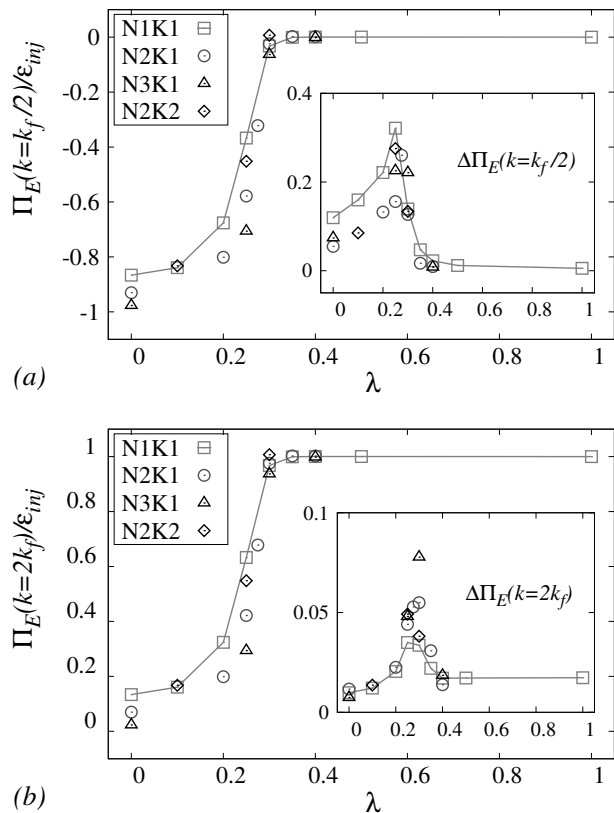


FIG. 4: Normalized energy flux at a scale larger (top) and smaller (bottom) than the forcing range versus  $\lambda$ . Insets show the fluctuations around the mean values. A guiding curve through data points is shown for N1K1.

ward cascade ( $|\Pi(k_f/2)|/\varepsilon_{inj} = 0$  and  $\Pi(2k_f)/\varepsilon_{inj} = 1$ ) is observed for values  $\lambda > \lambda_c$ . When  $Re$  and  $k_f$  are increased, the amplitude of the inverse cascade for the points in the range  $0 < \lambda < \lambda_c$  is increasing approaching the value  $|\Pi(k_f/2)|/\varepsilon_{inj} = 1$ , while the forward cascade is decreasing approaching the value  $\Pi(2k_f)/\varepsilon_{inj} = 0$ . The latter finding suggests that at infinite  $Re$  and  $k_f$  the cascade is unidirectional and inverse for  $\lambda < \lambda_c$ , while it is unidirectional and forward for  $\lambda > \lambda_c$ . The transition is thus discontinuous. This is at difference with what observed in quasi-2D systems where the transition occurs in a continuous manner (by a bidirectional cascade) similar to a second order phase transition, and at difference with what was observed in Ref. [24] where the transition occurred at a singular value of their model parameter,  $\alpha \sim 1$ .

This abrupt transition can be justified by realizing that in a bidirectional cascade the two inertial ranges ( $k_\mu \ll k \ll k_f$  and  $k_f \ll k \ll k_\nu$ ) must have different physical properties to sustain different directions of cascade. This is possible when, a new dimensional length scale  $\ell_*$  is introduced (e.g.,  $\ell_*$  is the layer thickness in thin layer turbulence, or the Zeeman scale in rotating

flows) that determines the properties of the flow due to the external mechanism. The amplitude of the inverse or forward cascade then depends on the ‘distance’ of the forcing scale  $\ell_f$  from the critical length scale  $\ell_*$ . In our case, no particular scale  $\ell_*$  is introduced by the parameter  $\lambda$ . On the contrary, the inertial ranges are scale invariant for all values of  $\lambda$ . Thus, both ranges,  $\ell > \ell_f$  and  $\ell < \ell_f$ , effectively share the same properties and have to develop either a forward or a backward cascade, because the flow can not distinguish the large from the small scales.

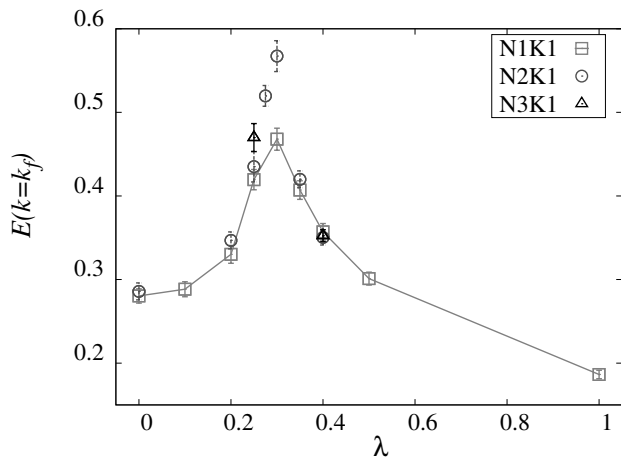


FIG. 5: Energy content at a wavenumber inside the forcing range ( $k = 11$ ) versus  $\lambda$ . We plot a guiding curve through data points for N1K1.

Not surprisingly, the system displays interesting behavior close to the critical value  $\lambda_c$ . In Fig. 5 we plot  $E(k_f)$ , the intensity of the spectrum at the forcing wavenumbers versus  $\lambda$  and for different Reynolds numbers. The response of the system is critical, showing a tendency for  $E(k_f)$  to diverge as  $\lambda \rightarrow \lambda_c$ . This divergence is also reflected in the amplitude of the flux fluctuations  $\Delta\Pi$  shown in the inset of Fig. 4 (where  $\Delta\Pi$  of run N2K2 is multiplied by  $2^{3/2}$  to account for the  $2^3$  more interactions involved). The existence of multiple phases for the physics of the energy containing eddies is an important remark that finds support also in recent experimental empirical findings where turbulent realizations with multiple states have been observed in swirling and in Taylor-Couette flows [27, 28].

The direction of the energy transfer can also be studied by looking at the behavior of the structure functions  $S_n(r) = \langle (\delta\mathbf{u}_{\parallel}(r))^n \rangle$ , where  $\delta\mathbf{u}_{\parallel}(r) = (\mathbf{u}(\mathbf{x} + \mathbf{r}) - \mathbf{u}(\mathbf{x})) \cdot \mathbf{r}/r$ , that have the advantage of being easily measured in experiments. In particular, for the original NSE, the von Kármán-Howarth equation states that the third order structure function is related to the direction of the cascade and it is negative for a forward transfer and positive for a backward transfer. In the form of the NSE investigated here [Eq. (1)], the von Kármán-Howarth equation is more complicated (see, e.g., Appendix A.1

of Ref. [23] for the case with  $\lambda = 0$ ). Nevertheless, we show in Fig. 6 that even a simple measurement based on  $S_3(r)$  is in good agreement with the indication that for  $r > r_f = 2\pi/k_f$  the sign does change by crossing  $\lambda_c$ .

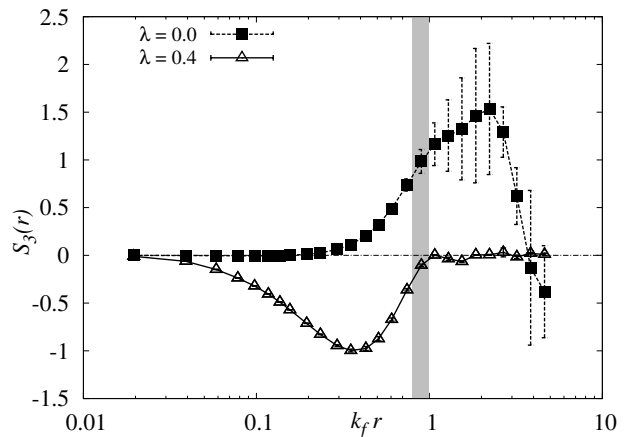


FIG. 6: Third order structure functions for the two cases with only direct or inverse energy cascade  $\lambda = 0.4$  and  $\lambda = 0$ .

In this work we have demonstrated that by controlling the amplitude of the interactions in the NSE the energy cascade can change direction from forward to inverse and *vice versa*. In the model used here, this change of direction is not due to previously known mechanisms, e.g., a change in the dimensionality, a change in the ideal invariants, or the breaking of any symmetry of the original equations caused by the introduction of external forcing as in the presence of rotation or of a magnetic field, revealing that the fully nonlinear dynamics of the 3D NSE is more complex than what was told by the accepted phenomenology. In particular, we showed that the energy cascade is strongly sensitive to the relative dynamical weight of homochiral to heterochiral helical Fourier interactions, suggesting the search for similar footprints of inverse energy transfer also in other empirical turbulent realization.

The mechanisms revealed here could be relevant to physical systems. In the case of rotation, the eigenmodes of the linear operator are in fact the helical modes used here, with the different sign helical modes having opposite direction of propagation. It is thus possible (although it still needs to be shown) that opposite helicity modes decorrelate faster and the relevant nonlinearities quench faster than same helicity modes. Similar properties might be at play in magnetohydrodynamics and in active fluids [29, 30].

Our results indicate that the transition becomes discontinuous in the large  $Re$  limit. This is the first time that such a discontinuous transition has been reported for the cascade direction. We have linked this discontinuity of the transition with the preservation of scale similarity in our model; thus, the same arguments can

also be applied to other out-of-equilibrium systems with scale similarity that do not originate from the NSE.

The presence of a control parameter in the turbulence model is key also to validate or benchmark the analytical theory of turbulence, e.g., renormalization group approaches or closures [31–34]. Our work thus points to a new direction in which the NSE (for  $\lambda = 1$ ) can be viewed as a system ‘close’ to criticality (for which  $\lambda = \lambda_c$ ) that can lead to new theoretical investigations in strongly out-of-equilibrium statistical mechanics.

The research leading to these results has received funding from the European Union’s Seventh Framework Programme (FP7/2007-2013) under grant agreement No. 339032.

- 
- [1] U. Frisch, *Turbulence: The Legacy of A. N. Kolmogorov* (Cambridge University Press, Cambridge, England, 1995).
- [2] A. Brissaud, U. Frisch, J. Leorat, M. Lesieur, and A. Mazure, *Phys. Fluids* **16**, 1366 (1973).
- [3] Q. Chen, S. Chen, and G. L. Eyink, *Phys. Fluids* **15**, 361 (2003).
- [4] L. M. Smith and F. Waleffe, *Phys. Fluids* **11**, 1608 (1999).
- [5] A. Celani, S. Musacchio, and D. Vincenzi, *Phys. Rev. Lett.* **104**, 184506 (2010).
- [6] A. Alexakis, *Phys. Rev. E* **84**, 056330 (2011).
- [7] A. Pouquet and R. Marino, *Phys. Rev. Lett.* **111**, 234501 (2013).
- [8] R. Marino, P. D. Mininni, D. Rosenberg, and A. Pouquet, *Europhys. Lett.* **102**, 44006 (2013).
- [9] E. Deusebio, G. Boffetta, E. Lindborg, and S. Musacchio, *Phys. Rev. E* **90**, 023005 (2014).
- [10] K. Seshasayanan, S. J. Benavides, and A. Alexakis, *Phys. Rev. E* **90**, 051003 (2014).
- [11] K. Seshasayanan and A. Alexakis, *Phys. Rev. E* **93**, 013104 (2016).
- [12] S. J. Benavides and A. Alexakis, *ArXiv e-prints* (2017), arXiv:1701.05162.
- [13] L. Biferale, F. Bonaccorso, I. M. Mazzitelli, M. A. T. van Hinsberg, A. S. Lanotte, S. Musacchio, P. Perlekar, and F. Toschi, *Phys. Rev. X* **6**, 041036 (2016).
- [14] H. Xia, D. Byrne, G. Falkovich, and M. Shats, *Nature Physics* **7**, 321 (2011).
- [15] E. Yarom, Y. Vardi, and E. Sharon, *Phys. Fluids* **25**, 085105 (2013).
- [16] A. Campagne, B. Gallet, F. Moisy, and P.-P. Cortet, *Phys. Fluids* **26**, 125112 (2014).
- [17] D. Byrne and J. A. Zhang, *Geophys. Res. Lett.* **40**, 1439 (2013).
- [18] A. Craya, *Sci. Tech. du Ministere de l’Air* (France) (1958).
- [19] J. Herring, D. Schertzer, M. Lesieur, G. Newman, J. Chollet, and M. Larcheveque, *J. Fluid Mech.* **124**, 411 (1982).
- [20] M. Lesieur, *Turbulence in Fluids* (Springer, The Netherlands, 2008).
- [21] F. Waleffe, *Phys. Fluids* **4**, 350 (1992).
- [22] L. Biferale, S. Musacchio, and F. Toschi, *Phys. Rev. Lett.* **108**, 164501 (2012).
- [23] L. Biferale, S. Musacchio, and F. Toschi, *J. Fluid Mech.* **730**, 309 (2013).
- [24] G. Sahoo, F. Bonaccorso, and L. Biferale, *Phys. Rev. E* **92**, 051002 (2015).
- [25] M. Kessar, F. Plunian, R. Stepanov, and G. Balarac, *Phys. Rev. E* **92**, 031004 (2015).
- [26] A. Alexakis, *J. Fluid Mech.* **812**, 752 (2017).
- [27] S. G. Huisman, R. C. Van Der Veen, C. Sun, and D. Lohse, *Nat. Commun.* **5** (2014).
- [28] P.-P. Cortet, A. Chiffaudel, F. Daviaud, and B. Dubrulle, *Phys. Rev. Lett.* **105**, 214501 (2010).
- [29] M. Linkmann, G. Sahoo, M. McKay, A. Berera, and L. Biferale, *Astrophys. J.* **836**, 26 (2017).
- [30] J. Stomka and J. Dunkel, *Proc. of the Natl. Acad. Sci.* **114**, 2119 (2017).
- [31] L. Canet, B. Delamotte, and N. Wschebor, *Phys. Rev. E* **93**, 063101 (2016).
- [32] M. J. Giles, *J. Phys. A: Mathematical and General* **34**, 4389 (2001).
- [33] V. S. L’vov and I. Procaccia, *Phys. Rev. E* **62**, 8037 (2000).
- [34] L. T. Adzhemyan, N. V. Antonov, and A. N. Vasil’ev, *The Field Theoretic Renormalization Group in Fully Developed Turbulence* (Gordon & Breach, London, 1999).